

Original Article

Tardigrade Augean stables—a challenging phylogeny and taxonomy of the family Ramazzottiidae (Eutardigrada: Hypsibioidea)

Pritam K. Dey^{1–3}, Alejandro López-López¹, Witold Morek¹, Łukasz Michalczyk^{1,*}

¹Department of Invertebrate Evolution, Institute of Zoology and Biomedical Research, Faculty of Biology, Jagiellonian University, Gronostajowa 9, 30-387 Kraków, Poland

²Doctoral School of Exact and Natural Sciences, Jagiellonian University, Łojasiewicza 11, 30-348 Kraków, Poland

³Natural History Museum of Denmark, University of Copenhagen, Universitetsparken 15, DK-2100, Copenhagen, Denmark

*Corresponding author. Department of Invertebrate Evolution, Institute of Zoology and Biomedical Research, Faculty of Biology, Jagiellonian University, Gronostajowa 9, 30-387 Kraków, Poland. E-mail: LM@tardigrada.net

ABSTRACT

Tardigrade taxonomy is most often hindered by prevalent outdated species descriptions, lack of integrative redescriptions, scarce genetic information, and fragmentary sampling. Here, we diagnose the problems obscuring phylogenetic inference and the taxonomy of the cosmopolitan family Ramazzottiidae. We carried out the most extensive phylogenetic analysis of this family to date, with a considerable influx of new genetic data from poorly sampled regions of the world. We found two new distinct evolutionary lineages defined by distinct morphological traits (dorsal cuticular sculpturing and/or body shape), characterized by restricted geographic distributions, and we delineated them as new species complexes: the Neotropical *Ramazzottius baumanni* complex and the Afro-Oriental *Ramazzottius szeptyckii* complex. Nevertheless, we could not confidently ascertain the taxonomic status of both complexes due to: (i) the current state of the ramazzottiid taxonomy, with outdated and/or imprecise species descriptions with heterogeneous terminology and, in many cases, without accounting for intraspecific variation; (ii) the missing genetic information for key taxa; and (iii) the possible lack of monophyly of *Cryoconicus* and *Ramazzottius* as suggested by our results. In addition to diagnosing the problems of ramazzottiid phylogeny and systematics, we also propose possible solutions that could accelerate the progress in our understanding of the evolution of this group.

Keywords: *Cryoconicus*; biogeography; DNA; integrative taxonomy; *Ramazzottius baumanni* complex; *Ramazzottius saltensis*; *Ramazzottius szeptyckii* complex; systematics; Tardigrada

INTRODUCTION

Tardigrades are bilateral micrometazoans (max 1.2 mm in length) that have four pairs of legs ending with sharp claws or digits (e.g. Nelson *et al.* 2018). They are also called water bears and are well known for their capability to withstand harsh environmental conditions (e.g. Hashimoto and Kunieda 2017). Tardigrades can be found from the bottom sediments of the ocean floor (e.g. Kaczmarek *et al.* 2015) to high mountain ranges such as the Himalayas (e.g. Kristensen 1987). Mosses and lichens are the most studied habitats in which these tiny creatures live, giving them the alternative name of moss piglets. Systematically, tardigrades comprise the phylum Tardigrada, which is most closely related to arthropods and onychophorans, all of them

included within the megaclass Ecdysozoa (Aguinaldo *et al.* 1997, Edgecombe *et al.* 2011).

Ramazzottius oberhaeuseri (Doyère, 1840) is the type species for *Ramazzottius* Binda and Pilato, 1986, the type genus for the family Ramazzottiidae. The species, originally named ‘*Macrobiotus oberhauseri*’, was among the first formally described tardigrade taxa. Eight years after the description, Ehrenberg (1848) transferred the species from *Macrobiotus* to a newly erected genus *Hypsibius* Ehrenberg, 1848. Almost 150 years later, *Hypsibius* species with claws I–IV of the *oberhaeuseri*-type, a pair of cephalic elliptical organs, and apophyses for the insertion of the stylet muscles in the shape of asymmetrical ‘blunt hooks’ were assigned to a newly erected *Ramazzottius* (Binda

and Pilato 1986). Based on an 18S rRNA phylogeny, Sands *et al.* (2008) transferred *Ramazzottius* and the closely related *Hebesuncus* Pilato, 1987 from the family Hypsibiidae to a new family, Ramazzottiidae. Recently, a third genus, *Cryoconicus* Zawierucha *et al.*, 2018, was added to the family.

The great majority of ramazzottiid species are represented by the members of the genus *Ramazzottius*, currently composed of 29 species, followed by *Hebesuncus* and *Cryoconicus*, each with four known species (Degma and Guidetti 2009–23). Whereas *Ramazzottius* has been reported from all continents and *Hebesuncus* has been recorded from all of them except Africa, *Cryoconicus* is known only from several disjunct localities, all characterized by a cold climate, such as montane and polar habitats (McInnes 1994, Biserov 1997–8, Zawierucha *et al.* 2018, Guidetti *et al.* 2019a). *Ramazzottius* and *Hebesuncus* were erected based solely on morphological traits and their validity has been further confirmed via molecular phylogenetics in several studies (Sands *et al.* 2008, Guil and Giribet 2012, Bertolani *et al.* 2014, Stec *et al.* 2018). In contrast, *Cryoconicus* has been delineated under the integrative taxonomy framework, although using a very limited genetic dataset (Zawierucha *et al.* 2018), so its validity should be verified with a larger number of ramazzottiid sequences.

Despite the wide distribution, ubiquity, and diversity of ramazzottiid species, our knowledge on the phyletic relationships within the family is very limited. The main reason for this state is the scarcity of type genetic data and mostly outdated species descriptions with unstandardized terminology describing cuticular sculpturing, one of the key taxonomic characters in the group. On the other hand, there are a number of ramazzottiid DNA sequences that are accompanied only by fragmentary morphological information (Stec *et al.* 2018) or without any associated phenotypic data (Jørgensen and Kristensen 2004, Guil and Giribet 2012; and numerous unpublished data from GenBank). In fact, only for a total of six ramazzottiid species (16%) is there a tandem of detailed morphological and genetic data available: *Ramazzottius oberhaeuseri* (Doyère, 1840) (in Stec *et al.* 2018), *Ramazzottius subanomalous* (Biserov, 1985) (in Stec *et al.* 2016 and 2017), *Ramazzottius sabatiniae* Guidetti, Massa *et al.*, 2019 (in Guidetti *et al.* 2019a), *Ramazzottius kretschmanni* Guidetti *et al.*, 2022 (in Guidetti *et al.* 2022), *Cryoconicus kaczmareki* Zawierucha *et al.*, 2018 (in Zawierucha *et al.* 2018), and *Cryoconicus antiarktos* Guidetti *et al.*, 2019 (in Guidetti *et al.* 2019a). Moreover, many of the ramazzottiid sequences deposited in GenBank are short, or are misidentified as *R. oberhaeuseri* (for details, see: Stec *et al.* 2018). Finally, the available DNA sequences are characterized by a strong bias in geographic sampling. Specifically, the great majority of them come from the Holarctic, with only occasional data obtained in the Polar regions, and with other parts of the world being blank spots on the map of ramazzottiid genetic diversity.

This is the first study focusing on a phylogenetic analysis of the family Ramazzottiidae, with a considerable influx of new genetic data from poorly sampled regions of the world. We use published data as well as new DNA sequences linked with morphology (observed both in light and scanning electron microscopy) for a considerable number of populations collected from three continents: Africa, South America, and Asia (these are the first ramazzottiid genetic data for the first two continents).

In addition to uncovering two distinct species complexes within *Ramazzottius* with the potential to become genera of their own, we also identify a number of challenges of ramazzottiid systematics, stemming from both natural and human causes, and potential ways to overcome them.

MATERIALS AND METHODS

Sampling and specimens

We analysed a total of 41 new *Ramazzottius* populations isolated from moss and lichen samples collected in three continents: South America (Neotropics), Africa (Afrotropic), and Asia (Orient); zoogeographic realms according to Holt *et al.* (2013). From each population, we selected a series of specimens that were independently used for the different experiments: phase contrast microscopy (PCM), scanning electron microscopy (SEM), and molecular analyses; for detailed information about the sample collection details and the number of specimens used for each of these analyses, see Table 1. The samples were examined according to the protocol described by Dastych (1980a) with modifications in Stec *et al.* (2015). After extraction, the samples were air dried and kept in the same envelope for further extractions, if necessary in the future. All the analysed samples, specimens, and vouchers were deposited in the Institute of Zoology and Biomedical Research, Jagiellonian University (Kraków, Poland). For morphological comparisons, we examined 14 phase contrast photomicrographs of two paratypes of *Ramazzottius baumanni* (Ramazzotti 1962) from the Ramazzotti collection deposited in the Natural History of Verona (Italy), kindly taken and sent to us by Professor Roberto Guidetti, and 88 phase contrast photomicrographs of nine specimens of *Ramazzottius saltensis* (Claps and Rossi 1984) [slide M20/6 (one holotype, seven paratypes) and slide M20/16 (one paratype)] from the Claps and Rossi collection deposited in the Museo de La Plata (La Plata, Buenos Aires, Argentina), kindly taken and sent to us by Dr Cristina Damborenea.

Microscopy, imaging, and DNA sequencing

Specimens were mounted in Hoyer's medium following the protocol described in detail in Morek *et al.* (2016), and then observed and photographed with an Olympus BX53 microscope with PCM and an Olympus DP74 digital camera. Specimens for imaging in SEM were prepared according to Stec *et al.* (2015) and examined under high vacuum in a Versa 3D DualBeam SEM at the ATOMIN facility of the Jagiellonian University, Kraków, Poland. All figures were assembled in Corel Photo-Paint 2018. For deep structures that could not be fully focused in a single light microscope photograph, a series of two to four images were taken every c. 0.2 µm and then assembled into a single deep-focus image by using Helicon Focus, v.8.2.0, with manual corrections wherever required.

DNA was extracted individually from one to seven (three on average) specimens per population, from a total of 19 populations, following the Chelex 100 resin (Bio-Rad) extraction method by Casquet *et al.* (2012), with modifications by Stec *et al.* (2020). Prior to DNA extraction, all specimens were mounted on temporary water slides and observed under a light microscope. After the extraction, if found in the vial,

Table 1. Collection details of populations analysed in this study. Analysis types: PCM, number of specimens fixed on permanent slides in Hoyer's medium for imaging in PCM; SEM, number of specimens on stubs for imaging in SEM; DNA, number of specimens processed for DNA extraction (the number of specimens from which DNA was successfully amplified is given in round brackets, whereas the number of recovered voucher is given in square brackets).

Sample code	Locality	Coordinates, altitude	Environment	Sample type	Specimens analysed		
					PCM	SEM	DNA
AR.190	South America, Argentina, Patagonia, vicinity of Lago Palena	43°58'22"S, 71°31'30"W, 970 m a.s.l.	forest	lichen	4	0	2 (2) [1]
AR.206		43°58'24"S, 71°31'35"W, 986 m a.s.l.	forest	lichen	1	4	0 (0) [0]
AR.227	South America, Argentina, Patagonia, vicinity of Tecka	43°27'49"S, 71°32'37"W, 700 m a.s.l.	shrubland	lichen	3	0	0 (0) [0]
AR.255	South America, Argentina, Patagonia, vicinity of El Bolsón	41°55'46"S, 71°33'23"W, 373 m a.s.l.	forest	moss	2	0	0 (0) [0]
AR.256		41°55'46"S, 71°33'24"W, 373 m a.s.l.	forest	moss	1	0	0 (0) [0]
AR.323	South America, Argentina, vicinity of San Miguel de Tucumán	26°52'12"S, 65°25'30"W, 855 m a.s.l.	forest	lichen	3	1	3 (3) [1]
AR.353	South America, Argentina, vicinity of Uruguay River	27°46'15"S, 55°04'25"W, 94 m a.s.l.	forest	lichen	15	3	3 (3) [1]
AR.365		27°46'10"S, 55°04'28"W, 93 m a.s.l.	forest	lichen	1	0	0 (0) [0]
AR.430	South America, Argentina, vicinity of Campina de América	26°16'58"S, 53°46'58"W, 652 m a.s.l.	rural	moss + lichen + algae	7	0	1 (1) [0]
AR.440		26°17'24"S, 53°46'29"W, 751 m a.s.l.	rural	lichen	1	0	0 (0) [0]
AR.446		26°17'23"S, 53°46'29"W, 749 m a.s.l.	rural	moss + lichen	4	0	1 (1) [0]
AR.466	South America, Argentina, Chaco, Bermejo Department	26°54'08"S, 58°42'14"W, 55 m a.s.l.	wetland forest	lichen	23	12	2 (2) [0]
AR.467		26°54'13"S, 58°42'15"W, 57 m a.s.l.	wetland forest	lichen	39	14	7 (3) [4]
AR.468		26°54'12"S, 58°42'14"W, 57 m a.s.l.	wetland forest	lichen	20	0	1 (1) [0]
AR.469		26°54'12"S, 58°42'15"W, 57 m a.s.l.	wetland forest	lichen	4	2	3 (3) [2]
AR.471		26°54'11"S, 58°42'12"W, 56 m a.s.l.	wetland forest	lichen	21	0	1 (1) [0]
AR.472		26°54'11"S, 58°42'14"W, 58 m a.s.l.	wetland forest	lichen	2	0	1 (1) [0]

Table 1. Continued

Sample code	Locality	Coordinates, altitude	Environment	Sample type	Specimens analysed		
					PCM	SEM	DNA
AR.475		26°54'12"S, 58°42'14"W, 67 m a.s.l.	wetland forest	lichen	4	0	0 (0) [0]
AR.483		26°54'09"S, 58°42'12"W, 55 m a.s.l.	wetland forest	lichen	8	2	2 (1) [0]
IN.302	Asia, India, Kerala, Idukki, Kannan Devan Hills	10°08'20"N, 77°06'10"E, 1969 m a.s.l.	tea plantation	moss + lichen	2	0	0 (0) [0]
IN.379	Asia, India, Tamil Nadu, Nilgiris, Doddabetta	11°24'46"N, 76°44'04"E, 2436 m a.s.l.	tea plantation	moss + lichen	1	0	0 (0) [0]
IN.387	Asia, India, Tamil Nadu, Nilgiris, Kattabettu	11°24'59"N, 76°49'08"E, 1995 m a.s.l.	tea plantation	moss + lichen	4	3	3 (2) [3]
ZA.131	Africa, Republic of South Africa, Eastern Cape, Valley Bushveld Country Lodge	33°37'34"S, 25°26'04"E, 222 m a.s.l.	shrubland	lichen	2	0	2 (2) [1]
ZA.145	Africa, Republic of South Africa, KwaZulu-Natal, vicinity of Kokstad	30°31'28"S, 29°40'43"E, 1315 m a.s.l.	forest	moss + lichen	0	0	2 (2) [0]
ZA.146		30°31'28"S, 29°40'43"E, 1315 m a.s.l.	forest	moss	1	0	0 (0) [0]
ZA.150		30°31'26"S, 29°40'44"E, 1342 m a.s.l.	forest	moss + lichen	0	1	1 (1) [0]
ZA.184	Africa, Republic of South Africa, KwaZulu-Natal, Drakensberg National Park, Giants Castle Game Reserve	29°03'26"S, 29°24'00"E, 1746 m a.s.l.	montane grassland	moss	1	0	0 (0) [0]
ZA.195		29°03'51"S, 29°23'33"E, 1962 m a.s.l.	montane grassland	moss + lichen	8	5	3 (3) [0]
ZA.208		29°03'30"S, 29°22'57"E, 1791 m a.s.l.	montane grassland	moss	1	0	0 (0) [0]
ZA.214		29°03'03"S, 29°24'07"E, 1517 m a.s.l.	forest	lichen	3	0	0 (0) [0]
ZA.216		29°02'59"S, 29°24'17"E, 1501 m a.s.l.	forest	moss + lichen	3	0	0 (0) [0]
ZA.224		29°16'08"S, 29°30'38"E, 1803 m a.s.l.	montane grassland	moss + lichen	1	0	0 (0) [0]
ZA.247		29°45'14"S, 29°11'33"E, 1905 m a.s.l.	riverside	lichen	2	0	0 (0) [0]
ZA.256		29°45'12"S, 29°11'17"E, 1942 m a.s.l.	riverside	moss	3	0	0 (0) [0]
ZA.362	Africa, Republic of South Africa, Eastern Cape, vicinity of Grahamstown	33°19'59"S, 26°32'37"E, 708 m a.s.l.	shrubland	moss	1	0	1 (1) [1]

Table 1. Continued

Sample code	Locality	Coordinates, altitude	Environment	Sample type	Specimens analysed		
					PCM	SEM	DNA
ZA.363		33°19'59"S, 26°32'36"E, 703m a.s.l.	shrubland	moss + lichen	1	0	0 (0) [0]
ZA.367		33°20'00"S, 26°32'41"E, 688 m a.s.l.	shrubland	lichen	7	0	3 (3) [0]
ZA.370		33°20'00"S, 26°32'35"E, 692 m a.s.l.	shrubland	moss + lichen	2	0	0 (0) [0]
ZA.529	Africa, Republic of South Africa, Western Cape, Jonkershoek Nature Reserve	34°00'19"S, 18°59'37"E, 543 m a.s.l.	mountains	moss + lichen	1	0	0 (0) [0]
ZA.534		34°00'21"S, 18°59'45"E, 614 m a.s.l.	mountains	moss + lichen	1	0	0 (0) [0]
ZA.538		34°00'21"S, 18°59'45"E, 614 m a.s.l.	mountains	moss	1	0	0 (0) [0]

exoskeletons were mounted on permanent microscope slides as voucher specimens, regardless of whether the DNA amplification was successful (see Table 1 for details of the number of specimens from which DNA was successfully amplified and the number of recovered vouchers mounted on permanent slides). Four molecular markers, three nuclear and one mitochondrial, were sequenced using Sanger sequencing: the small ribosomal subunit (18S rRNA), the large ribosomal subunit (28S rRNA), the second internal transcribed spacer (ITS2), and the subunit I of the cytochrome *c* oxidase (COI). Primer and polymerase chain reaction (PCR) protocol details are listed in Table 2. The sequences were manually checked, cleaned, and corrected in GENEIOUS (available from www.geneious.com).

Phylogenetic analysis

Phylogenetic analyses were carried out using three nuclear markers (18S rRNA, 28S rRNA, and ITS2). The COI sequences were not used for the phylogenetic analyses, as the taxon coverage was highly unbalanced and their inclusion in preliminary analyses decreased node supports. We added sequences from *Ramazzottius* and related genera available in GenBank to our dataset (accession numbers are listed in the Supporting Information, SM.01). The sequences were aligned independently for each marker, using MAFFT (Katoh and Standley 2013). The alignments were checked in GENEIOUS and trimmed to 811 (18S rRNA), 787 (28S rRNA), 488 (ITS2) bp, removing terminal portions with a high level of missing data or low-quality bases. We created two different matrices concatenating the individual fragments: one including all three markers, and another including only the 18S rRNA and the 28S rRNA fragment.

Maximum likelihood phylogenetic analyses were carried out for each of our matrices in IQTREE 1.6.10 (Nguyen et al. 2015), searching for the most appropriate partition scheme

(Chernomor et al. 2016) and model (Kalyaanamoorthy et al. 2017), and including an ultrafast bootstrap with 1000 replicates (Hoang et al. 2018). Bayesian inference analyses were carried out in MrBayes 3.2.6 (Ronquist and Huelsenbeck 2003), running for 5 million generations, sampling a tree each 5000 generations, and discarding the first 25% of trees as burn-in. The matrix was partitioned for each analysis, with each partition corresponding to each marker.

Species identification and denotation

Specimens for which no morphological data are available are designated as 'Ramazzottius sp.', i.e. they could represent both known and undescribed taxa. Specimens morphologically similar to the described species with outdated descriptions are denoted as uncertain identifications ('cf.'), e.g. *Ramazzottius* cf. *baumanni* indicates specimens that probably represent *Ramazzottius baumanni*, but the quality of the original description and type series, as well as the lack of type DNA sequences, prevent a confident identification of the species. Specimens that do not correspond to any of the described species and can be assigned to one of the species complexes are denoted jointly with an 'aff.' and an 'sp. can.' ('species candidatus'/'candidate species') abbreviations, e.g. *Ramazzottius* aff. *baumanni* sp. can. indicates an undescribed candidate species representing the *baumanni* complex. This way much more information about the species affinity and status (known/unknown) can be derived compared to the very voluminous denotation of 'Ramazzottius sp.'. Importantly, the 'sp. can.' denotation is not equivalent to a nomenclatural act of erecting a new species, which includes naming the species, providing its detailed description, designating a type series, type locality, etc.. Thus, using the 'sp. can.' denotation does not violate the International Code of Zoological Nomenclature.

Table 2. Primers and references for amplification protocols of the four DNA fragments sequenced in the study.

DNA fragment	Primer name	Primer direction	Primer sequence (5'-3')	Primer source	PCR programme
18S rRNA	18S_Tar_Ff1	forward	AGGC GAA ACC CGCAATGGCTC	Stec et al. (2017)	Zeller (2010)
	18S_Tar_Rr2	reverse	CTGATCGCCTTCGAACCTCTAACTTCG		
28S rRNA	28S_Eutar_F	forward	ACCCGCTGAACCTTAAGCATAT	Gąsiorek et al. (2017)	Mironov et al. (2012)
	28SR0990	reverse	CCTTGGTCCGTGTTCAAGAC		
ITS2	ITS2_Eutar_Ff	forward	CGTAACGTGAATTGCAGGAC	Stec et al. (2018)	Stec et al. (2018)
	ITS2_Eutar_Rr	reverse	TGATATGCTTAAGTTCAGCGG		
COI	LCO1490_JJ	forward	CHACWAAYCATAAAGATATYGG	Astrin and Stüben (2008)	Folmer et al. (1994)
	HCO2198_JJ	reverse	AWACTTCVGGRTGVCCAAARAATCA		

RESULTS

Molecular phylogeny

In general, the phylogenetic trees did not show optimal values for clade support, and the topology of the tree varied depending on the number of taxa included and the number of markers analysed (Supporting Information SM.02). The tree that was built based on a 18S rRNA + 28S rRNA + ITS2 matrix and that included all taxa for which at least the 18S rRNA or the 28S rRNA sequence was available, was characterized by the highest, although still only moderate, support values (Fig. 1). Similar results were obtained in both IQTREE and MrBayes. In further tests, in which we analysed subsets of the matrix (removing sequences for which only one marker was available, or removing sequences without associated morphological data, analysing each marker separately) to rule out artefacts caused by incorrect or chimeric sequences, the relationships between the clades, and the taxa within each clade, were found to be variable, but the monophyly of the three main clades (overwhelmingly Holarctic *Ramazzottius* s.s. + cryophilic *Cryoconicus*, Neotropical *Ramazzottius*, and Afro-Oriental *Ramazzottius*) was always recovered, except in a few cases in which the matrix was drastically reduced and the clades became polyphyletic. In some of these analyses, the sequences corresponding to the genus *Hebesuncus* were recovered within the *Ramazzottius* lineages, and in some cases *Hebesuncus* was paraphyletic or polytomous relative to *Ramazzottius* + *Cryoconicus*.

Therefore, here, we interpret the phylogenetic tree obtained from analysing the complete matrix with IQTREE (Fig. 1), which had the highest relative support values. Specifically, in this tree, all analysed representatives of the family Ramazzottiidae formed a very well-supported clade (sister to *Hypsibius* in the analysed dataset). Within ramazzottiids, six well-supported clades, all in a polytomous relationship, were recovered: the *Hebesuncus* clade, and five lineages that comprised all analysed *Ramazzottius* and *Cryoconicus* specimens. The first clade, mostly Holarctic but with two Antarctic species, comprised about eight *Ramazzottius* species, including morphologically characterized *R. oberhaeuseri* (the type species for the genus), *R. sabatiniae*, *R. subanomalus*, and *R. varieornatus*, as well as about four species that are not linked with publicly available phenotypic data, some misidentified as '*R. oberhaeuseri*'. At the base of the first clade, two *Cryoconicus* species, paraphyletic to each other and in relation to *Ramazzottius* clade A, were present (*C. antiarktos* was collected in the Antarctic, whereas *C. kaczmareki*, the type

species for the genus, was found in the Holarctic, close to the border with the Sino-Japanese realm). The next two lineages (*Ramazzottius* clades B and C) were represented by about two to three Holarctic species without publicly available phenotypic data, some misidentified as '*R. oberhaeuseri*'. The fourth *Ramazzottius* clade was entirely Neotropical and represents the *Ramazzottius baumanni* complex (see the next section for the morphological diagnosis), comprising three preliminarily delineated and identified species: *R. cf. baumanni* and *R. aff. baumanni* sp. can. in a sister-relationship, and *R. cf. saltensis*. Finally, the fifth clade comprised the Afro-Oriental *Ramazzottius szepetynkii* complex (see the next section for the morphological diagnosis) and consisted of four species in a paraphyletic relationship: *Ramazzottius szepetynkii* (Dastych, 1980) in Dastych (1980b) (from the Afrotropic) and an additional three tentatively delineated new species (two collected in the Afrotropic and one in the Oriental realm).

Concise morphological characterization of the *Ramazzottius* clades A–C

Ramazzottius clade A

This clade comprises four species of *Ramazzottius* with well-described morphology and a further four genetically delineated species with no or limited published phenotypic data. The species for which morphology has been described, exhibit *oberhaeuseri*-type body shape (i.e. slim) and unknown or purple to reddish-brown pigmentation (dissolvable in Hoyer's). Eyes absent (in alive animals). There are two cephalic elliptical organs poorly visible under PCM and clearly visible under SEM. Pigmentation on the dorsum with chequered pattern present (*R. oberhaeuseri*, *R. subanomalus*, and *R. varieornatus*) or unknown (*R. sabatiniae*). Dorsal cuticle smooth (e.g. *R. subanomalus*), smooth to weakly sculptured with flat polygons (e.g. *R. oberhaeuseri* and *R. sabatiniae*) or strongly sculptured with granular polygons (e.g. *R. varieornatus*). Cephalic elliptical organs poorly to well visible under PCM and always clearly visible under the SEM. Bucco-pharyngeal apparatus and claws of the *Ramazzottius* type. Egg processes vary in shape and could be hemispherical, conical, thorn, spine, or filamentous and sometimes ended with a rounded tip or flattened enlargements. Surface of the egg finely dotted (e.g. *R. varieornatus*) or smooth (e.g. *R. oberhaeuseri*, *R. subanomalus*, and *R. sabatiniae*) under PCM but finely wrinkled (e.g. *R. oberhaeuseri*) under SEM.

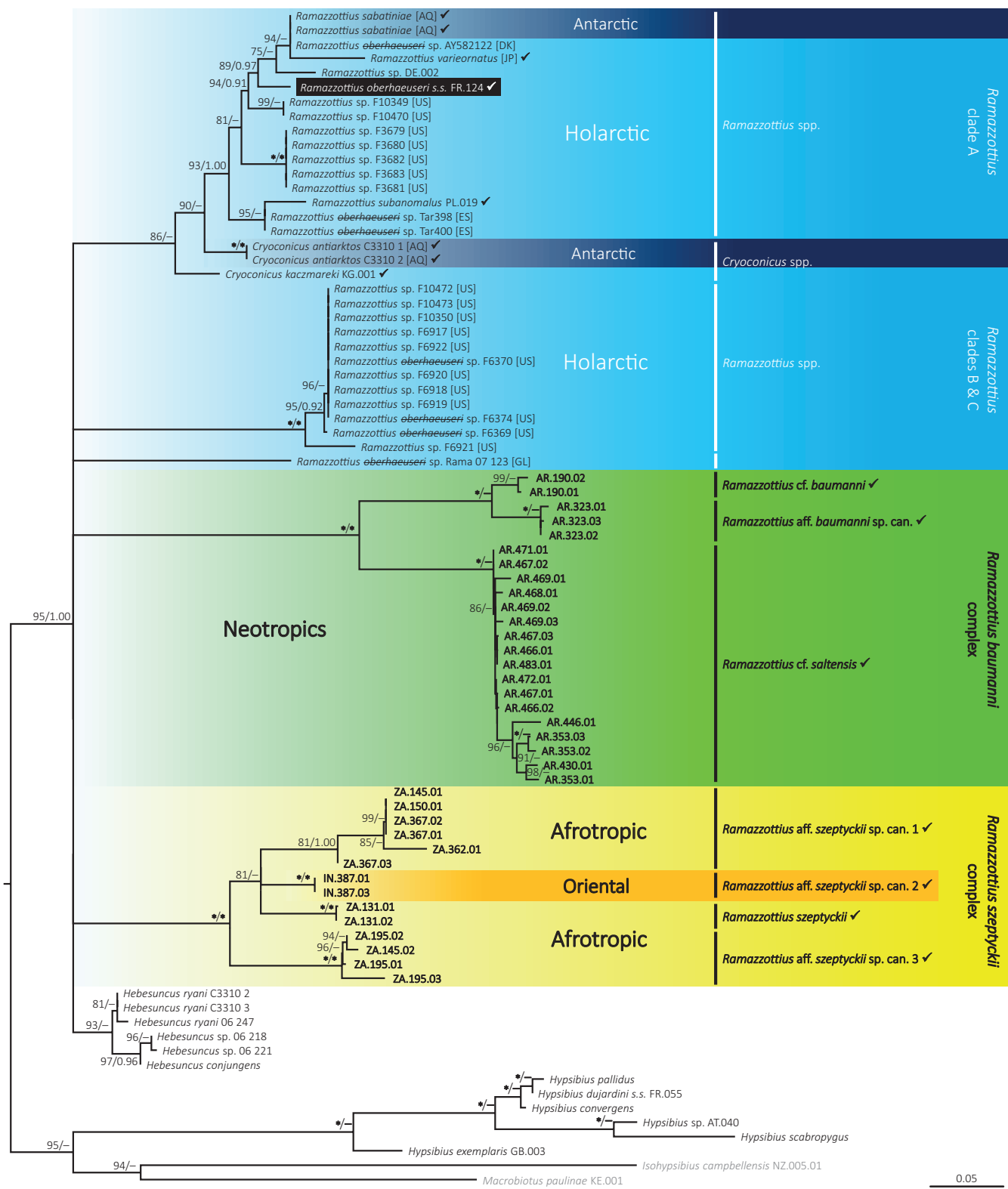


Figure 1. Phylogenetic tree of the Ramazzottiid family obtained in IQTREE from a matrix with concatenated 18S rRNA, 28S rRNA, and ITS2 markers. All sequences identified in GenBank as ‘*R. oberhaeuseri*’ but not clustering with the neotype sequence (highlighted in black) in one clade, are labelled here as ‘*Ramazzottius oberhaeuseri* sp.’, with the specific epithet crossed out to reduce the spread of erroneous taxonomic identifications. Nodes with low support (bootstrap < 75) have been collapsed. Values above nodes indicate bootstrap support values (left) and posterior probability (right); posterior probability is given only if the node was recovered in the MRBAYES tree and/or its value was > 0.9; maximal values are denoted with asterisks (*). Taxa for which morphological data are publicly available are marked with a tick mark (✓). Newly sequenced populations, species and complexes are bolded. Background shading colours indicate zoogeographical realms in which the analysed populations were collected.

Ramazzottius clades B and C

There are no phenotypic data currently available for these two clades, which are composed by unvouchered sequences obtained from GenBank.

Delineation of new species complexes in *Ramazzottius*

We analysed a total of new 41 *Ramazzottius* populations: 19 from the Neotropics (Argentina), 19 from the Afrotropic (Republic of South Africa), and three from the Oriental realm (India). We found a correlation between dorsal sculpturing and/or body shape (Figs 2–5; Tables 3, 4) and the molecular phylogeny (Fig. 1). Based on this integrative analysis, below we diagnose two new species complexes: the Neotropical clade as the *Ramazzottius baumanni* species complex (Figs 2, 3; Table 3) and the Afro-oriental clade as the *Ramazzottius szeptyckii* species complex (Figs 4, 5; Table 4).

The Ramazzottius baumanni complex

Body shape of the *oberhaeuseri*-type. Body colour pinkish-red to reddish-brown. Eyes absent (in alive animals). Two cephalic elliptical organs usually clearly visible under PCM and always in SEM. Dorsal cuticle strongly sculptured with elevated polygons and sclerotized apexes (see below for the details). Buccopharyngeal apparatus and claws of the *Ramazzottius* type. Eggs unknown.

The *R. baumanni* complex exhibits unique dorsolateral sculpturing, although it may be mistaken at first sight with the sculpture of some species in the *R. oberhaeuseri* complex. In both cases, there are transverse bands across the dorsolateral cuticle covered with a more or less polygonal pattern, but its character differs between the two groups. In the *R. oberhaeuseri* complex, the pattern is created by clearly separated flat or slightly rounded polygonal tubercles (flat polygons, see: Stec et al. 2018). However, in some species, such as in *Ramazzottius agannae* Dastych, 2011, the polygons can be elevated, which makes the pattern more pronounced. Nevertheless, the polygons and spaces between them seem to be covered with a cuticle of a similar thickness (polygon edges are darker in PCM, because the polygon wall is observed from above, meaning that the light travels through a larger amount of cuticular matter compared to the polygon ceiling). In the *R. baumanni* complex (Figs 2, 3), however, the transverse bands are covered with tightly packed granules with a different level of sclerotization of their apices. Thus, the polygonal pattern is created either by an evident thickening of the apical part of each granule (*R. cf. baumanni* and *R. aff. baumanni* sp. can.) or by a contact of bases and walls of neighbouring granules (*R. cf. saltensis*). In the last case, the sculpturing may look like a reticulum in PCM at first, as the granule walls in contact form a dark reticulate pattern, with central parts of granules appearing as brighter ‘meshes’. However, a more careful inspection reveals that there are spaces within the ‘reticulum’ where granules are not in contact and that the central parts of ‘meshes’ are dimmed, which suggests a thicker cuticle (this dimming is caused by a partial sclerotization of the granule apex; Fig. 2F, insert). When observed in SEM (Fig. 3), there is no doubt that the entire dorsolateral cuticle (including areas between the transverse bands) is covered with granules (i.e. there are no signs of reticulation or flat polygonal sculpture). In all analysed species, granule bases are wide and covered with microgranulation,

whereas granule apices protrude higher, are not covered with microgranulation and may be smooth or wrinkled. The sculptured transverse dorsolateral bands may exhibit undulation (PCM), which in SEM is visible as weakly outlined gibbosities.

Apart from *R. baumanni*, *R. saltensis*, and the new Neotropic species tentatively delineated in this study (Figs 2, 3), *Ramazzottius belubellus* Bartels et al., 2011 (known from the Nearctic) is also assigned to the *R. baumanni* complex based on the cuticular sculpturing, pending genetic verification (granules in this species are usually in the shape of high cones with sharp apices). Main qualitative differences between the species of the complex are listed in Table 3.

Ramazzottius cf. baumanni (Figs 2A, B, 3A–C)

Specimens/populations analysed: 15/5 [11 specimens on microscope slides: AR.190.03–4; AR.206.02; AR.227.02; AR.255.01; AR. 256.01 + 1 voucher on slide: Ram.cf.bau_AR.190.01 + 4 specimens on SEM stub 22.14]. Eight evident transverse dorsolateral bands with evident granulation. Smaller granules are also present on the entire head and between the transverse bands. Granule apices strongly sclerotized: pebble-shaped (often with ragged edges), dark (non-translucent) in PCM (Fig. 2B) and pebble- or cone-shaped with an almost smooth surface in SEM (Fig. 3C). In PCM, the transverse bands appear undulated (Fig. 2A), but in SEM weakly developed gibbosities in lateral positions are visible (Fig. 3A). Pigmentation dissolves in Hoyer’s medium. Eggs unknown.

Specimens analysed in this study generally fit the original description of *R. baumanni*, compared to the two examined paratypes (see Supporting Information, SM.03). However, our specimens have a very distinct dark granulation under PCM. Although this might be caused by the medium and/or the age of the slides, we decided to remain conservative until topotype DNA sequences from the type locality are available, hence the uncertain (‘cf.’) identification of our material.

Ramazzottius aff. baumanni sp. can. (Figs 2C, D, 3D–F)

Specimens/populations analysed: 4/1 [three specimens on microscope slides: AR.323.01–2 + 1 voucher on slide: Ram. aff.bau.sp.can._AR.323.01 + 1 specimen on SEM stub 22.16]. Seven evident transverse dorsolateral bands with evident granulation, with occasional very small and sparse granules on legs II and III, remaining parts of the cuticle smooth. Granule apices strongly sclerotized: pebble-shaped (with smooth edges), dark (non-translucent) in PCM (Fig. 2D) and pebble-shaped with an evidently wrinkled surface in SEM (Fig. 3F). No undulations or gibbosities are visible either in PCM (Fig. 2C) or SEM (Fig. 3D). Dorsolateral pigmentation clearly visible in the form of pseudoplate-like structures, in specimens mounted in Hoyer’s medium, under both the granulated transverse bands and the patches of smooth cuticle. Eggs unknown.

The species differs from *R. baumanni* by fewer dorsolateral bands of granulation (seven vs. eight), smaller and more numerous dorsal granules, the lack of granulation on the head and on legs, the presence of pigmented pseudoplate-like pattern in specimens fixed in Hoyer’s medium, and by the lack of undulations/gibbosities on the transverse bands. Moreover, the DNA analysis confirmed that it represents a distinct evolutionary lineage (Fig. 1).

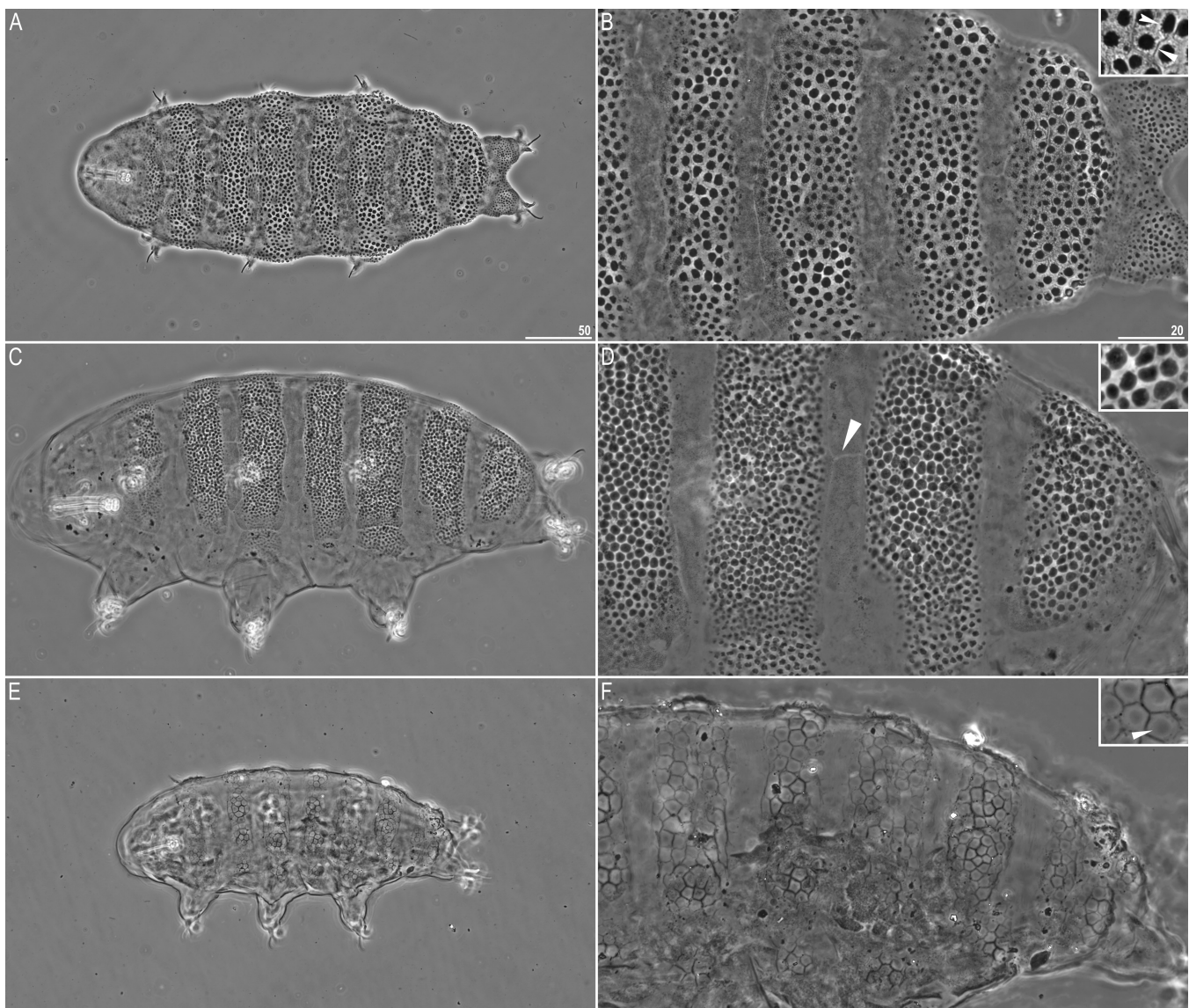


Figure 2. The *Ramazzottius baumannii* species complex—morphological variability in dorsal cuticular sculpturing between the three species delineated in the present study, as seen in PCM (all photographs, except for inserts, obtained from stacking multiple images taken in the Z-axis). The left column shows entire specimens, whereas the right one shows magnified caudodorsal parts of the cuticle (photos in columns taken under the same magnification). A, B, *Ramazzottius cf. baumannii* (slide AR.190.04), the insert shows a magnified cuticle fragment with dark borders between the bases of adjacent granules (the flat arrowhead) and ragged edges of the sclerotized apices of the granules (the indented arrowhead); C, D, *Ramazzottius aff. baumannii* sp. can. (slide AR.323.01), the flat arrowhead indicates a pseudoplate-like structures formed by dorsal pigmentation, the insert shows a magnified cuticle fragment with strongly sclerotized process apices; E, F, *Ramazzottius cf. saltensis* (slide AR.467.01), the insert shows a magnified cuticle fragment with weakly sclerotized process apices (the flat arrowhead). All specimens are paragenophores. Scale bars in μm .

Ramazzottius cf. saltensis (Figs 2E, F, 3G–I)

Specimens/populations analysed: 182/13 [149 individuals on microscope slides: AR.353.03–4; AR.365.01; AR.430.01–2, 06–7; AR.440.02; AR.446.02–3; AR.466.03; AR.467.01,03; AR.468.04; AR.469.02; AR.471.01,05; AR.472.01; AR.475.02–3; AR.483.02 + 7 vouchers on slides: Ram.cf.sal_AR.353.01; Ram.cf.sal_AR.467.02–04, 07; Ram.cf.sal_AR.469.01, 03 + 33 individuals on SEM stubs 22.11–5; populations: AR.353, AR.466, AR.467, AR.469 and AR.483]. Eight evident transverse dorsolateral bands with evident, large, bubble-like granulation. Granulation on the head, all legs, and between the transverse

rows also present, but weakly developed (smaller and more sparsely distributed granules). In PCM, granules appear densely packed, so the walls of adjacent granules form a pseudoreticulum; granule apices are weakly sclerotized, so they appear only slightly dimmed compared to the less sclerotized parts around the apex; the sclerotized apex portion with fuzzy edges. In SEM, granule apices are in the shape of flattened domes with a strongly wrinkled surface. In PCM, the transverse bands appear undulated (Fig. 2E), but in SEM weakly developed gibbosities are visible (Fig. 3G). Development of granulation and gibbosities on the transverse bands varies widely among specimens. Eggs unknown.

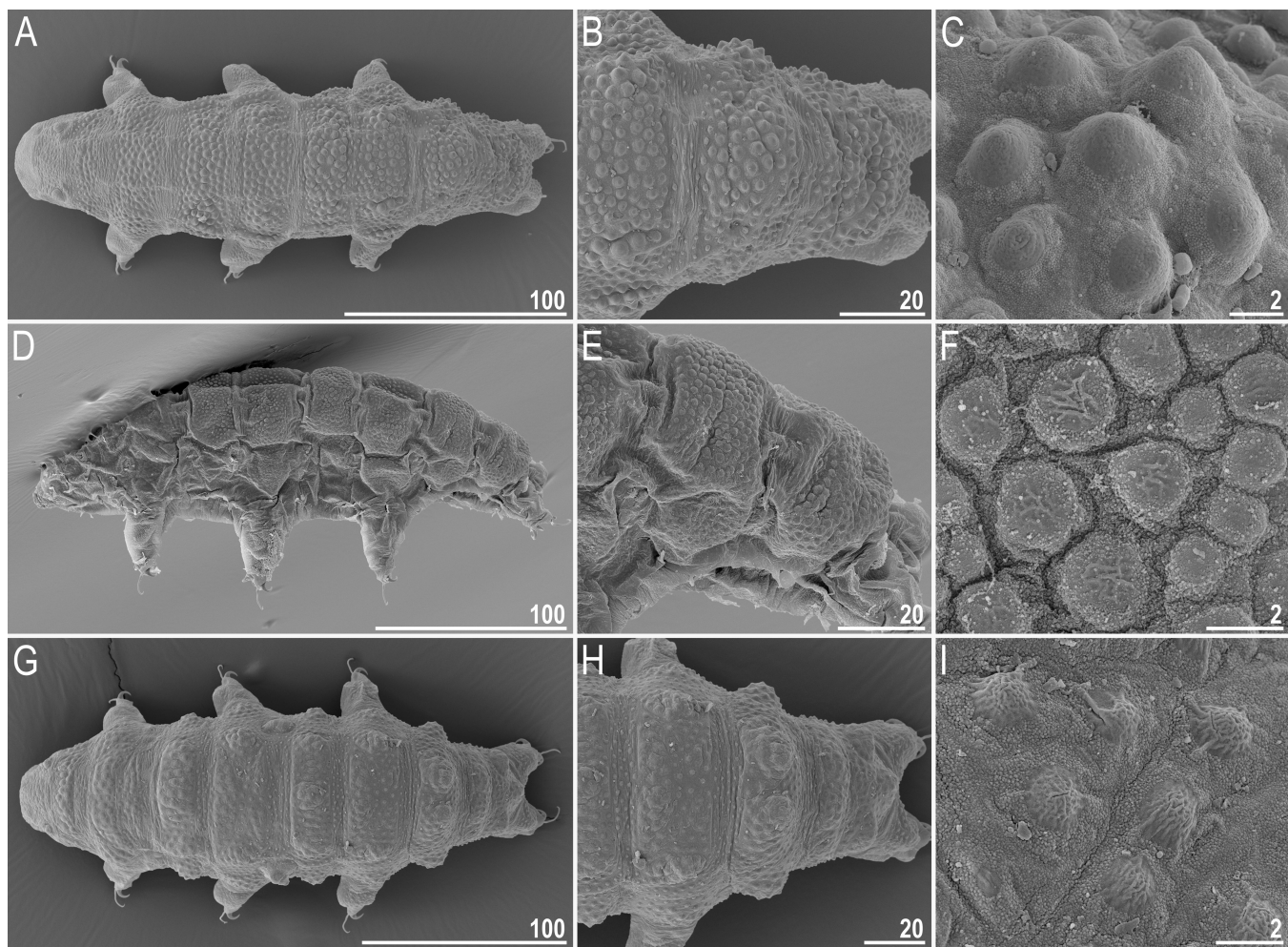


Figure 3. The *Ramazzottius baumannii* species complex—morphological variability in dorsal cuticular sculpturing between the three species delineated in the present study, as seen in SEM. The left column shows entire specimens, whereas the middle one shows magnified caudodorsal parts of the cuticle and the right one shows details of granulation morphology. A–C, *Ramazzottius cf. baumannii* (stub 22.14); D–F, *Ramazzottius aff. baumannii* sp. can. (stub 22.16); G–I, *Ramazzottius cf. saltensis* (stub 22.13). Scale bars in μm .

Specimens analysed in this study generally fit the original description of *R. saltensis*, but not all taxonomically important traits are clearly visible in the type series (see Supporting Information, SM.03). Thus, we decided to remain conservative until topotype DNA sequences from the type locality are available, hence the uncertain (cf.) identification of our material.

The Ramazzottius szeptyckii complex

Body shape of the *szeptyckii* type (corpulent/toad-like), except for *R. aff. szeptyckii* sp. can. 3 (which has the *oberhaeuseri*-type body shape). Body colour reddish-brown to brown. Eyes absent (in alive animals). Two cephalic elliptical organs are clearly visible under the PCM and SEM. Dorsolateral gibbosities present, reticulated or smooth, but never with polygonal granulation. Bucco-pharyngeal apparatus and claws of the *Ramazzottius* type. Eggs unknown.

Species in the *R. szeptyckii* complex differ from all other known *Ramazzottius* species by a corpulent (toad-like) body shape and/or by the presence of dorsolateral gibbosities, and from the *baumannii* complex by the lack of cuticular granulation. Depending on the species, the surface of gibbosities can be reticulated, wrinkled,

or smooth. Moreover, there is a considerable interspecific (and sometimes also some intraspecific) variation in gibbosity prominence. Apart from *R. szeptyckii*, we have tentatively identified four new species in the complex: three integratively, and one based on morphology (Figs 4, 5). Main qualitative differences between the species of the complex are listed in Table 4.

Ramazzottius szeptyckii (Fig. 4A, B)

Specimens/populations analysed: 15/7 (microscope slides: ZA.131.01; ZA.184.03; ZA.214.01; ZA.216.03–4; ZA.224.04; ZA.247.01, ZA.256.01–2 + 1 voucher on slide: Ram.sze_ZA.131.01). Body corpulent. Gibbosities prominent, with an evidently reticulated surface. Eggs unknown.

The species has been described based only a single individual (i.e. there are no data on the intraspecific variability) and no type DNA sequences are available. Thus, an identification of this species is difficult. Nevertheless, overall, our specimens fit the original description of *R. szeptyckii*. Moreover, despite an extensive sampling (more than 500 samples collected) in the Republic of South Africa, the *terra typica* of the species, and recording a total of five species of the complex in the country, we found only one species fitting the

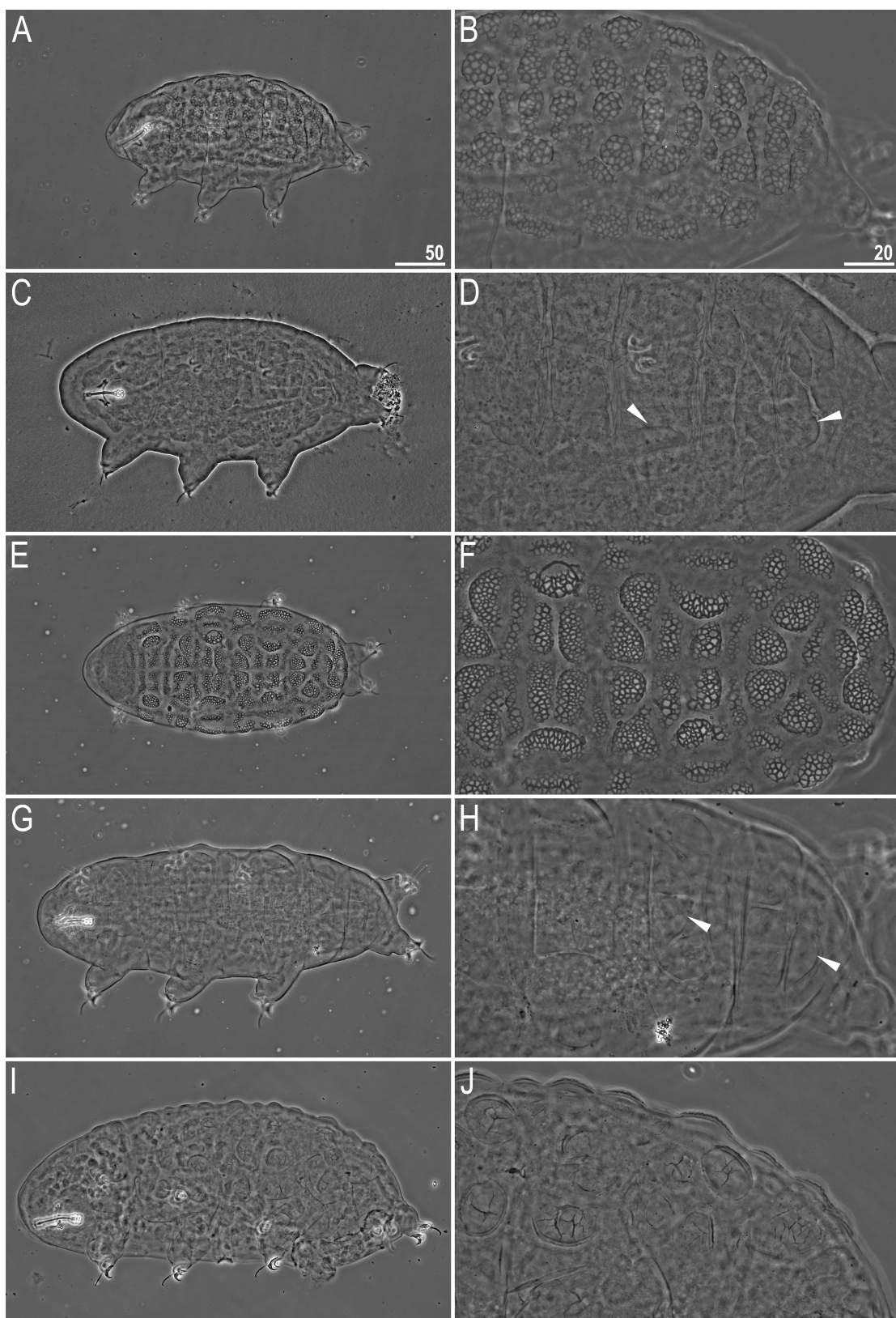


Figure 4. The *Ramazzottius szeptyckii* species complex—morphological variability in body shape and dorsal cuticular sculpturing between the five species delineated in the present study, as seen in PCM (all photographs obtained from stacking multiple images taken in the Z-axis). The left column shows entire specimens, whereas the right one shows magnified caudodorsal parts of the cuticle (photos in columns taken under the same magnification). A, B, *Ramazzottius szeptyckii* (slide ZA.131.01); C, D, *Ramazzottius aff. szeptyckii* sp. can. 1 (slide ZA.367.05); E, F, *Ramazzottius aff. szeptyckii* sp. can. 2 (slide IN.387.01); G, H, *Ramazzottius aff. szeptyckii* sp. can. 3 (slide ZA.195.01); I–J, *Ramazzottius aff. szeptyckii* sp. can. 4 (slide ZA.529.01). Arrowheads indicate weakly developed gibbosities. All specimens except the last one are paragenophores. Scale bars in μm.

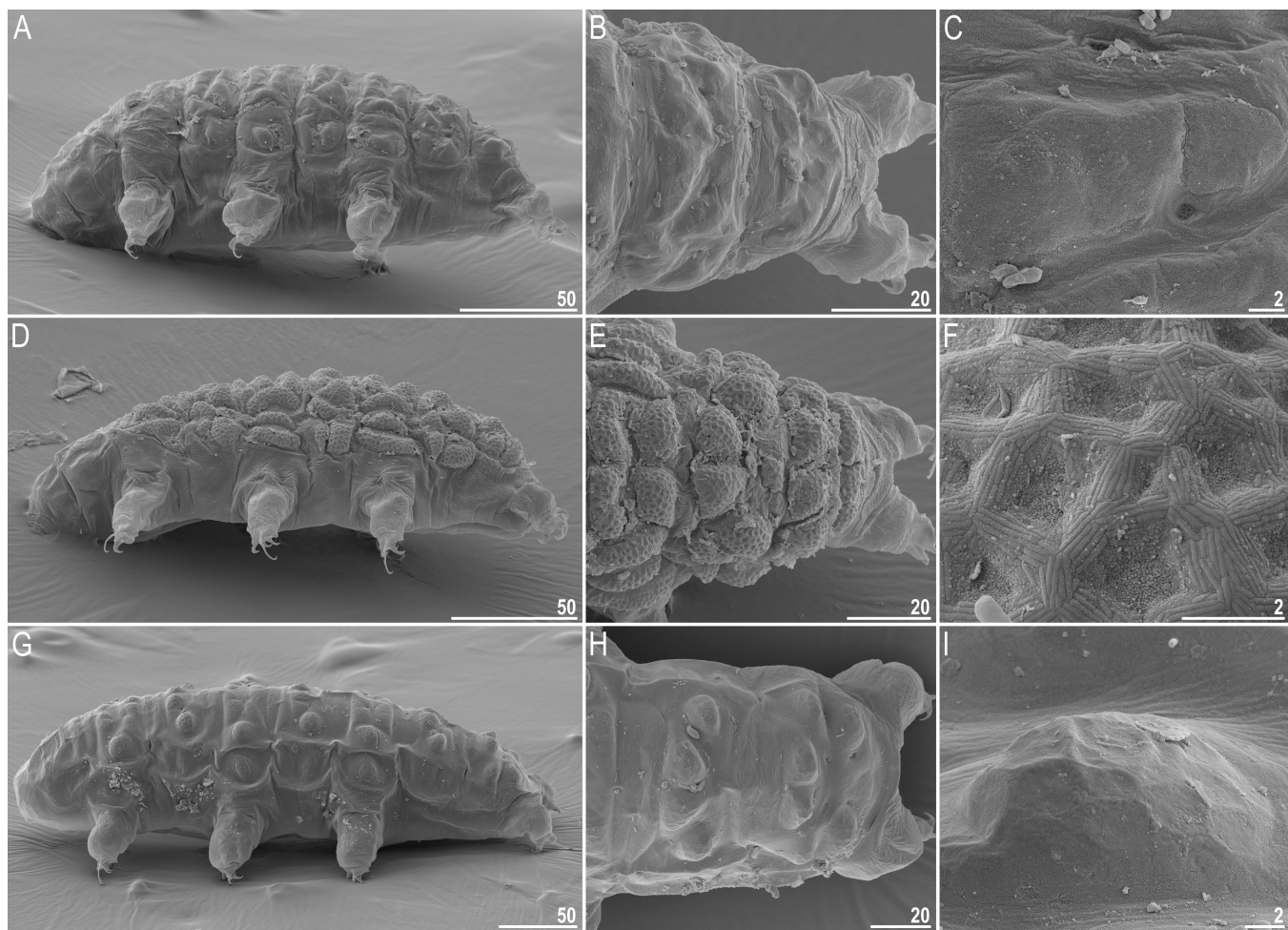


Figure 5. The *Ramazzottius szeptyckii* species complex—morphological variability in body shape and dorsal cuticular sculpturing between the three species delineated in the present study, as seen in SEM. The left column shows entire specimens in lateral view, whereas the middle one shows magnified caudodorsal parts of the cuticle and the right one shows details of gibbosity morphology. A–C, *Ramazzottius aff. szeptyckii* sp. can. 1 (stub 22.11); D–F, *Ramazzottius aff. szeptyckii* sp. can. 2 (stub 22.13); G–H, *Ramazzottius aff. szeptyckii* sp. can. 3 (stub 22.12). Scale bars in μm .

Table 3. The three species of the *Ramazzottius baumanni* complex identified with phenotypic and genetic data in the present study, in samples from South America. Details of cuticle morphology characterized as seen in PCM. Phylogenetic positions are based on a concatenated 18S rRNA + 28S rRNA + ITS2 nucleotide sequence set (see Fig. 1 for details) and key morphological traits (dorsolateral cuticle sculpturing) differentiating the species are provided.

Phylogenetic position	Species	Granule apex shape (in lateral view)	Granule apex sclerotisation (cuticle density-opacity)	Sclerotized apex boundary	Transverse band undulation
	<i>R. cf. baumanni</i>	rounded	strong	ragged	present (only laterally)
	<i>R. aff. baumanni</i> sp. can.	rounded	strong	sharp	absent
	<i>R. cf. saltensis</i>	rounded	weak	fuzzy	present
?	<i>R. belubellus</i>	pointy	intermediate	sharp	absent

original description of *R. szeptyckii*, which reduces the probability of our population representing a cryptic *R. szeptyckii*-like species.

Ramazzottius aff. szeptyckii sp. can. 1 (Figs 4C, D, 5A–C)

Specimens/populations analysed: 13/6 [12 individuals on microscope slides: ZA.146.02; ZA.208.01; ZA.362.02; ZA.363.01; ZA.367.05–6; ZA.370.01 + 1 voucher on slide;

Ram.aff.sze.sp.can.1_ZA.362.01 + 1 individual on SEM stub 22.11 (population ZA.150)] found together with *R. aff. szeptyckii* sp. can. 3 (sample ZA.145). Body corpulent. Gibbosities faint, more visible on the caudal part of the body, not visible at all in larger specimens in PCM (Fig. 4C, D); clearly visible in the only specimen observed in SEM (Fig. 5A–C). Gibbosities smooth. Eggs unknown.

Table 4. The five species of the *Ramazzottius szeptyckii* complex identified with phenotypic and/or genetic data in the present study, in samples from South Africa and a sample from India. Details of cuticle morphology characterized as seen in PCM. Phylogenetic positions are based on a concatenated 18S rRNA + 28S rRNA + ITS2 nucleotide sequence set (see Fig. 1 for details) and key morphological traits (body shape and gibbosity morphotype) differentiating the species are provided wherever available.

Phyletic position	Species	Body shape	Dorsolateral gibbosity prominence	Dorsolateral gibbosity surface
	<i>R. aff. szeptyckii</i> sp. can. 1	corpulent	faint	smooth
	<i>R. aff. szeptyckii</i> sp. can. 2	corpulent	prominent	reticulated
	<i>R. szeptyckii</i>	corpulent	prominent	reticulated
	<i>R. aff. szeptyckii</i> sp. can. 3	slim	faint	smooth
?	<i>R. aff. szeptyckii</i> sp. can. 4	corpulent	clearly outlined	wrinkled

Currently, this is the only reported *Ramazzottius* species with a corpulent body and smooth gibbosities. Moreover, the DNA analysis confirmed that it represents a distinct evolutionary lineage (Fig. 1).

Ramazzottius aff. szeptyckii sp. can. 2 (Figs 4E, F, 5D–F)

Specimens/populations analysed: 10/3 [7 individuals on microscope slides: IN.302.03–4; IN.379.02; IN.387.01–4 + 3 vouchers on slides: Ram.aff.sze.sp.can.2_IN.387.01–3 + 3 individuals on SEM stub: 22.13 (population IN.387)]. Body corpulent. Gibbosities prominent, with an evidently reticulated surface both in PCM (Fig. 4E, F) and SEM (Fig. 5D–F). Eggs unknown.

This new species is morphologically similar to *R. szeptyckii*, but differs from it by the mean maximal diameter of mesh of the gibbosity reticulation (*c.* 4.4 µm among 12 Hoyer-mounted specimens of *R. szeptyckii* vs. *c.* 3.2 µm among the seven Hoyer-mounted specimens *R. aff. szeptyckii* sp. can. 2; measured on the same three gibbosities: in the anterior, central, and posterior parts of the dorsum). Moreover, the DNA analysis confirmed that it represents a distinct evolutionary lineage collected from a different zoogeographic realm (Fig. 1).

Ramazzottius aff. szeptyckii sp. can. 3 (Figs 3G, H, 5G–I)

Specimens/populations analysed: 13/1 [eight individuals on microscope slides: ZA.195.01–2 + 5 individuals on SEM stub 22.12]; found together with *R. aff. szeptyckii* sp. can. 1 (sample ZA.145). Body slim (similar in shape to *R. oberhaeuseri*). Gibbosities faint, more visible on the caudal part of the body, poorly visible in larger specimens in PCM (Fig. 3G, H), but prominent in all five specimens examined in SEM (Fig. 5G–I). Gibbosity surface smooth in PCM and almost smooth in SEM (a reticulum-like scaffolding protrudes delicately through the cuticle). Eggs unknown.

Currently, this is the only reported *Ramazzottius* species with a slim body and smooth cuticle and gibbosities. Moreover, the DNA analysis confirmed that it represents a distinct evolutionary lineage (Fig. 1).

Ramazzottius aff. szeptyckii sp. can. 4 (Fig. 3I, J)

Specimens/populations analysed: 3/3 [microscope slides: ZA.529.01; ZA.534.01; ZA.538.02]. Body corpulent. Gibbosities seem to be weakly sclerotized, but they are clearly outlined and with an irregularly wrinkled surface. We were not

able to obtain DNA sequences for this species, hence its affinity to the complex is based solely on morphology. Eggs unknown.

Currently, this is the only reported *Ramazzottius* species with wrinkled gibbosities.

DISCUSSION

The new morphological and genetic data concerning *Ramazzottius* presented in this study shed some light on the evolution of the genus. However, at the same time, our work also highlights challenges of ramazzottiid phylogeny and systematics stemming from both biological and human-related causes.

Although the family Ramazzottiidae is cosmopolitan, which may seem to provide ample material for study, particular species are rare and, if found, they are often represented by a low numbers of individuals, which are not always accompanied by their eggs (often a source of key taxonomic traits in this tardigrade group). This considerably limits taxonomic inference, especially considering that both published data (Stec *et al.* 2016, 2017) and our current observations indicate that at least some species exhibit large intraspecific morphological variability. On the other hand, there probably are cases of species crypsis (Stec *et al.* 2018) caused by parallel evolution and/or morphological stasis, similarly to what has been observed in *Milnesium* (Morek and Michalczyk 2020). The combination of cases of high intra-specific and low interspecific morphological variability makes the taxonomy of the genus naturally challenging.

With the currently available data, the topology of the ramazzottiid tree is still too labile and highly dependent on the set of taxa and the number of markers included in the analysis, which suggests that the addition of new data may change the tree topology. This problem may be caused by the presence of missing data in our matrix (some markers could not be amplified or are not available for some taxa), lack of taxonomic representativeness (absence of data from some lineages that can help the phylogenetic algorithms to find the optimal topology), an insufficient number of variable sites for a matrix of this size, and/or by some characteristics of the markers, such as saturation or heterogeneity (Wiens 2003, 2006, Som 2015, Streicher *et al.* 2016, Dong *et al.* 2022). Finally, it is also possible that at least some of the difficulties in resolving ramazzottiid phylogenetic relationships may be caused by ancient periods of rapid lineage diversification and/or contrasting rates of evolution (adaptation) in different clades, which usually lead to the inference of incorrect

topologies (Wiens 2006, Som 2015). All of these issues may have caused the low support of basal nodes in our trees, the changing relationship between the *Ramazzottius* clades, and their relationships with *Cryoconicus* and *Hebesuncus*.

These problems currently preclude a division of *Ramazzottius* into separate genera, which would aid handling the constantly growing number of discovered ramazzottiid species. The unstable topology of the ramazzottiid phylogenetic tree, especially the unsolved relationships between the clades representing the two species complexes identified in this study, and the scarcity of genetic data for the family prevented us from erecting the *R. baumanni* and the *R. szeptyczkii* complexes as new genera, despite both groups seeming to exhibit sufficient morphological and genetic divergence. We decided to adopt a conservative approach also because our analyses question the validity of *Cryoconicus*, even though the genus exhibits clear apomorphies (e.g. elongated claws with the external/posterior primary branch detached from the claw base, apophyses for the insertion of the stylet muscles in the shape of two long crests, dark body colour; Zawierucha et al. 2018, Guidetti et al. 2019a). Specifically, it is not clear whether the genus is monophyletic and if it does not break the monophyly of *Ramazzottius*. The only two *Cryoconicus* species for which we have DNA sequences, *C. kaczmareki* and *C. antiarktos*, have been recovered either in a polytomous relationship with *Ramazzottius* (in: Guidetti et al. 2019a) or in a paraphyletic relationship, nested within *Ramazzottius* (in the present study; see Fig. 1). Nevertheless, given the unstable topology of the ramazzottiid phylogenetic tree, and the lack of morphological data for the *Ramazzottius* clades B and C, it would be premature to suppress *Cryoconicus*. The genus could be upheld if it adheres to the rules of natural classification, i.e. if future analyses return a stable topology in which *Cryoconicus* is monophyletic and is in a sister-relationship to *Ramazzottius*. The latter condition could also be met if the *R. baumanni* and/or the *R. szeptyczkii* complex, and/or the *Ramazzottius* clades B and C, are delineated as separate genera, and *Cryoconicus* is sister to the *Ramazzottius* clade A.

In parallel, the natural challenges of ramazzottiid systematics listed above are multiplied by the current state of ramazzottiid taxonomy. This is caused mainly by species descriptions, most of which are outdated. It has been explicitly shown in recent years that genetic data are crucial for accurate tardigrade species delineation and identification, especially when faced with cryptic and pseudocryptic species, taxa exhibiting considerable intraspecific variation, and in cases where more than one congeneric species are found in a single moss/lichen sample (Stec et al. 2016, 2018, Bartylak et al. 2019, Guidetti et al. 2019b, Morek et al. 2019, Surmacz et al. 2019, Gąsiorek et al. 2021a). Currently, there are type DNA sequences only for five of the currently recognized 37 ramazzottiid species (14%), and non-type genetic and morphological data are available for two species (5%) (including *R. szeptyczkii* reported in the present study). Thus, a considerable effort is needed to integratively redescribe the remaining majority of species. Given that many of them were reported only once and the type localities are scattered throughout the globe, this task is extremely difficult and would require Herculean efforts compared to providing integrative data when describing new species. In other words, this shows how important it is to avoid publishing species descriptions devoid of genetic markers

for aiding progress in our understanding of tardigrade diversity and evolution.

Apart from the lack of DNA sequences, most ramazzottiid species descriptions are based on a limited sample size. This usually provides very little insight into the extent of phenotypic intra- vs. interspecific variability, which are also essential for species delineation and identification. The limited knowledge on morphological variation is especially detrimental when coupled (which is usually the case) with missing genetic data. When type genetic sequences are available, it is easier to supplement the original species description with new phenotypic data, as new populations representing the species can be much more confidently assigned to that taxon using DNA barcoding than based on morphology, especially with a limited knowledge on its variability. A close-at-hand example of the difficulties caused by outdated species descriptions lacking genetic data are our uncertain identifications ('cf.') of two of the species of the *R. baumanni* complex. The inability to determine whether our specimens represent the already described species or new taxa impairs progress in describing Neotropical tardigrade diversity.

Furthermore, the history of ramazzottiid species descriptions, spanning over 180 years and numerous authors, has inevitably led to a confusing morphological terminology. Especially, the cuticular sculpturing provides ample examples both for how the same morphotype can be described with different words, and—on the other hand—how various structures can be named with a single term. For instance, the sculpture in the shape of flattened or slightly rounded polygons found in many ramazzottiid taxa has been termed as 'granulation', 'polygons', or 'tuberles' (e.g. Bisarov 1997–8, Kaczmarek et al. 2006, Pilato et al. 2013). On the other hand, the latter term has been used to describe gibbosities, distinct large or indistinct small flat polygons (e.g. Ramazzotti 1962, Dastych 1980b, Kaczmarek et al. 2006). This terminological inconsistency underlines the importance of the quality imaging in tardigrade species descriptions, which allows for direct comparisons in spite of the terminology.

Our study also indicates that another researcher-related factor, a long-lasting common conviction that tardigrade species are, by definition, cosmopolitan, may have also impeded the discovery of ramazzottiid diversity. This is evidenced, for example, by multiple DNA sequences (mis)identified as '*R. oberhaeuseri*' which are scattered across the *Ramazzottius* clades A–C (see Fig. 1). In contrast to this 'everything is everywhere' paradigm, we found an emerging biogeographic pattern suggesting that the analysed lineages could be geographically restricted. This is in line with recent zoogeographic analyses in other tardigrade groups, e.g. *Milnesium* in Morek et al. (2021), *Pseudechiniscus* in Gąsiorek et al. (2021b), or *Bryodelphax* in Gąsiorek et al. (2020). However, it needs to be noted that scarce sampling, such as in *Ramazzottius*, may result in retrieving false patterns. Thus, the biogeographic structure recovered in this study, however clear, must be considered as a preliminary result, which may become more complex when data for more species and populations are available.

Importantly, the results of this study allow not only for diagnosing problems with uncovering ramazzottiid evolution and building its systematics, but they also help to formulate solutions to these challenges and to get the ramazzottiid stables cleaned in order to eliminate the taxonomic impediment and to

better understand the evolution of this group. Considering the state of ramazzottiid taxonomy, we should make more effort to redescribe species (Stec *et al.* 2018), provide genetic and new morphological data for new populations representing described species (Stec *et al.* 2016, 2017), and to publish photographs of the original type series for species of which descriptions contained only drawings or poor quality images (for examples of studies providing such useful photomicrographs, see: Dastych 2009, Guidetti *et al.* 2019a, 2022). We should also try to clarify and unify the terminology used for the description of cuticular sculpturing, which seems to be a source of important taxonomic traits (scanning electron microscopy imaging will definitely help in reducing the probability of misinterpretations). In parallel, avoiding the publication of new species devoid of type DNA sequences is essential, not only to prevent a further build-up of taxonomic and biogeographic problems, but also to provide the very much desired data for a reliable reconstruction of the phylogeny of Ramazzottiidae.

SUPPLEMENTARY DATA

Supplementary data are available at *Zoological Journal of the Linnean Society* online.

ACKNOWLEDGEMENTS

African samples were collected under permits No: CN35-285316 issued by CapeNature, OP 3570/2018 issued by Ezemvelo KZN Wildlife. Indian samples were collected under permit no. NBA/Tech Appl/9/Form B/179/20/20-21/3891. We are grateful to Carol Simon (Stellenbosch University, RSA) for her invaluable help with the field sampling in South Africa, and to Bartek Surmacz (Agricultural University of Kraków, Poland) for his assistance during fieldwork in Africa and South America. We are very thankful to Professor Roberto Guidetti (University of Modena and Reggio Emilia, Modena, Italy) and Dr Cristina Damborenea (La Plata Museum, La Plata, Argentina) for sending us photos of type specimens of *R. baumannii* and *R. saltensis*, respectively. Thomas Pape (Natural History Museum of Denmark, University of Copenhagen, Denmark) is most heartily thanked for the discussion on the International Code of Zoological Nomenclature. We would also like to thank the reviewers for their valuable comments, which helped us to improve the manuscript.

FUNDING

This work was supported by the *Sonata Bis* programme (grant no. 2016/22/E/NZ8/00417 to Ł.M.) funded by the Polish National Science Centre.

CONFLICT OF INTEREST

The authors declare that they have no competing interests.

DATA AVAILABILITY

All data pertaining to this article are present in the body of the text, as Supporting Information files, or are deposited in GenBank.

REFERENCES

- Aguinaldo AM, Turbeville JM, Linford LS *et al.* Evidence for a clade of nematodes, arthropods and other moulting animals. *Nature* 1997;387:489–93.
- Astrin JJ, Stüben PE. Phylogeny in cryptic weevils: molecules, morphology and new genera of western Palaearctic Cryptorhynchinae (Coleoptera: Curculionidae). *Invertebrate Systematics* 2008;22:503–22.
- Bartels PJ, Nelson DR, Kaczmarek Ł *et al.* *Ramazzottius belubellus*, a new species of Tardigrada (Eutardigrada: Parachela: Hypsibiidae) from the Great Smoky Mountains National Park (North Carolina USA). *Proceedings of the Biological Society of Washington* 2011;124:23–7.
- Bartylak T, Kulpa A, Grobys D *et al.* Variability of *Echiniscus tristis* Gąsiorek & Kristensen, 2018—is morphology sufficient for taxonomic differentiation of Echiniscidae? *Zootaxa* 2019;4701:1–24.
- Bertolani R, Guidetti R, Marchioro T *et al.* Phylogeny of Eutardigrada: New molecular data and their morphological support lead to the identification of new evolutionary lineages. *Molecular Phylogenetics and Evolution* 2014;76:110–26.
- Binda MG, Pilato G. *Ramazzottius*, nuovo genere di Eutardigrado (Hypsibiidae). *Animalia* 1986;13:159–66.
- Biserov VI. *Hypsibus subanomalus* sp n (Eutardigrada, Hypsibiidae) from the Astrakhan District. *Zoologicheskii Zhurnal* 1985;64:131–5.
- Biserov VI. Tardigrades of the Caucasus with a taxonomic analysis of the genus *Ramazzottius* (Parachela: Hypsibiidae). *Zoologischer Anzeiger* 1997/98;236:139–59.
- Casquet J, Thebaud C, Gillespie RG. Chelex without boiling a rapid and easy technique to obtain stable amplifiable DNA from small amounts of ethanol-stored spiders. *Molecular Ecology Resources* 2012;12:136–41.
- Chernomor O, Haeseler AV, Minh BQ. Terrace aware data structure for phylogenomic inference from supermatrices. *Systematic Biology* 2016;65:997–1008.
- Claps MC, Rossi GC. Contribucion al conocimiento de los tardigrados de Argentina IV. *Acta Zoologica Lilloana* 1984;38:45–50.
- Dastych H. Niesporczaki (Tardigrada) Tatrzańskiego Parku Narodowego. *Monografie Fauny Polski* 1980a;9:1–232.
- Dastych H. *Hypsibus szepeticki* sp nov., a new species of Tardigrada from South Africa. *Bulletin of Polish Academic of Science* 1980b;27:505–8.
- Dastych H. Notes on the African limno-terrestrial tardigrade *Ramazzottius szepeticki* (Dastych, 1980) (Tardigrada). *Entomologische Mitteilungen aus dem Zoologischen Museum Hamburg* 2009;15:87–91.
- Dastych H. *Ramazzottius agannae* sp nov a new tardigrade species from the nival zone of the Austrian Central Alps (Tardigrada). *Entomologische Mitteilungen aus dem Zoologischen Museum Hamburg* 2011;15:237–53.
- Degma P, Guidetti R. *Actual Checklist of Tardigrada Species*, 2009–23. https://doi.org/10.25431/11380_1178608 (accessed 06/03/2023).
- Dong Z, Qu S, Landrein S *et al.* Increasing taxa sampling provides new insights on the phylogenetic relationship between *Eriobotrya* and *Rhaphiolepis*. *Frontiers in Genetics* 2022;13:831206.
- Doyère LMF. Memoire sur les Tardigrades I. *Annales des Sciences Naturelles, Paris, Series* 1840;2:269–362.
- Edgecombe GD, Giribet G, Dunn CW *et al.* Higher-level metazoan relationships: recent progress and remaining questions. *Organisms Diversity & Evolution* 2011;11:151–72.
- Ehrenberg CG. Fortgesetzte Beobachtungen über jetzt herrschende atmospharische mikroskopische, etc mit Nachtrag und Novarum Specierum Diagnosis. *Akademie des Wissenschaften, Monatsberichte, Berlin* 1848;13:370–81.
- Folmer O, Black M, Hoeh W *et al.* DNA primers for amplification of mitochondrial cytochrome c oxidase subunit I from diverse metazoan invertebrates. *Molecular Marine Biology and Biotechnology* 1994;3:294–9.
- Gąsiorek P, Stec D, Morek W *et al.* An integrative redescription of *Echiniscus testudo* (Doyère, 1840), the nominal taxon for the class Heterotardigrada (Ecdysozoa: Panarthropoda: Tardigrada). *Zoologischer Anzeiger* 2017;270:107–22.
- Gąsiorek P, Stec D, Zawierucha K *et al.* Revision of *Testechiniscus* Kristensen, 1987 (Heterotardigrada: Echiniscidae) refutes the polar-temperate distribution of the genus. *Zootaxa* 2018;4472:261–97.
- Gąsiorek P, Vončina K, Degma P *et al.* Small is beautiful: the first phylogenetic analysis of *Bryodelphax* Thulin, 1928 (Heterotardigrada: Echiniscidae). *Zoosystematics and Evolution* 2020;96:217–36.

- Gąsiorek P, Vončina K, Nelson DR et al. The importance of being integrative: a remarkable case of synonymy in the genus *Viridiscus* (Heterotardigrada: Echiniscidae). *Zoological Letters* 2021a;7:13.
- Gąsiorek P, Vončina K, Zająć K, Michalczyk Ł. Phylogeography and morphological evolution of *Pseudechiniscus* (Heterotardigrada: Echiniscidae). *Scientific Reports* 2021b;11:7606.
- Guidetti R, Massa E, Bertolani R et al. Increasing knowledge of Antarctic biodiversity: new endemic taxa of tardigrades (Eutardigrada; Ramazzottidae) and their evolutionary relationships. *Systematics and Biodiversity* 2019a;17:573–93.
- Guidetti R, Cesari M, Bertolani R et al. High diversity in species, reproductive modes and distribution within the *Paramacrobios richtersi* complex (Eutardigrada, Macrobiotidae). *Zoological Letters* 2019b;5:1.
- Guidetti R, Cesari M, Giovannini I et al. Morphology and taxonomy of the genus *Ramazzottius* (Eutardigrada; Ramazzottidae) with the integrative description of *Ramazzottius kretschmanni* sp nov. *The European Zoological Journal* 2022;89:346–70.
- Guil N, Giribet G. A comprehensive molecular phylogeny of tardigrades adding genes and taxa to a poorly resolved phylum-level phylogeny. *Cladistics* 2012;28:21–49.
- Hashimoto T, Kunieda T. DNA protection protein, a novel mechanism of radiation tolerance: lessons from tardigrades. *Life (Basel, Switzerland)* 2017;7:26.
- Hoang DT, Chernomor O, Haeseler AV et al. UFBoot2: improving the ultrafast bootstrap approximation. *Molecular Biology and Evolution* 2018;35:518–22.
- Holt BG, Lessard JP, Borregaard MK et al. An update of Wallace's zoogeographic regions of the World. *Science* 2013;339:74–8.
- Jørgensen A, Kristensen RM. Molecular phylogeny of Tardigrada—investigation of the monophyly of Heterotardigrada. *Molecular Phylogenetics and Evolution* 2004;32:666–70.
- Kaczmarek Ł, Michalczyk Ł, Diduszko D. *Ramazzottius bunikowskiae*, a new species of Tardigrada (Eutardigrada: Hypsibiidae) from Russia. *Zootaxa* 2006;1229:49–57.
- Kaczmarek Ł, Bartels PJ, Roszkowska M et al. The zoogeography of marine Tardigrada. *Zootaxa* 2015;4037:1–189.
- Kalyaanamoorthy S, Minh BQ, Wong T et al. ModelFinder: fast model selection for accurate phylogenetic estimates. *Nature Methods* 2017;14:587–9.
- Katoh K, Standley DM. MAFFT multiple sequence alignment software version 7: improvements in performance and usability. *Molecular Biology and Evolution* 2013;30:772–80.
- Kristensen RM. Generic revision of the Echiniscidae (Heterotardigrada), with a discussion of the origin of the family. In: Bertolani R (ed.), *Biology of Tardigrades. Selected Symposia and Monographs U.Z.I.* Modena (Italy): Mucchi Editore, 1987, 261–335.
- McInnes SJ. Zoogeographic distribution of terrestrial/freshwater tardigrades from current literature. *Journal of Natural History* 1994;28:257–352.
- Mironov SV, Dabert J, Dabert M. A new feather mite species of the genus *Proctophyllodes* Robin, 1877 (Astigmata: Proctophyllodidae) from the long-tailed tit *Aegithalos caudatus* (Passeriformes: Aegithalidae)—morphological description with DNA barcode data. *Zootaxa* 2012;3253:54–61.
- Morek W, Michalczyk Ł. First extensive multilocus phylogeny of the genus *Milnesium* (Tardigrada) reveals no congruence between genetic markers and morphological traits. *Zoological Journal of the Linnean Society* 2020;188:681–93.
- Morek W, Stec D, Gąsiorek P et al. An experimental test of eutardigrade preparation methods for light microscopy. *Zoological Journal of the Linnean Society* 2016;178:785–93.
- Morek W, Stec D, Gąsiorek P et al. *Milnesium tardigradum* Doyère, 1840: The first integrative study of interpopulation variability in a tardigrade species. *Journal of Zoological Systematics and Evolutionary Research* 2019;57:1–23.
- Morek W, Surmacz B, López-López A et al. 'Everything is not everywhere': time-calibrated phylogeography of the genus *Milnesium* (Tardigrada). *Molecular Ecology* 2021;30:3590–609.
- Nelson DR, Bartels PJ, Guil N. Tardigrade ecology. In: Schill RO (ed.), *Water Bears: the Biology of Tardigrades*. Cham: Springer, 2018, 163–210.
- Nguyen LT, Schmidt HA, Haeseler AV et al. IQ-TREE: a fast and effective stochastic algorithm for estimating maximum-likelihood phylogenies. *Molecular Biology and Evolution* 2015;32:268–74.
- Pilato G. Revision of the genus *Diphascon* Plate, 1989, with remarks on the subfamily Itaquasconinae (Eutardigrada, Hypsibiidae). In: Bertolani R. (ed.), *Biology of Tardigrades. Selected Symposia and Monographs U.Z.I.* Modena (Italy): Mucchi Editore, 1987, 337–357.
- Pilato G, D'Urso V, Lisi O. *Ramazzottius thulini* (Pilato, 1970) bona species and description of *Ramazzottius libycus* sp nov (Eutardigrada, Ramazzottidae). *Zootaxa* 2013;3681:270–80.
- Ramazzotti G. Tardigradi del Cile con descrizione di quattro nuove specie e di una nuova varietà. *Atti della Società Italiana di Scienze Naturali Museo Civico di Storia Naturale Milano* 1962;101:275–87.
- Ronquist F, Huelsenbeck JP. MrBayes 3: Bayesian phylogenetic inference under mixed models. *Bioinformatics* 2003;19:1572–4.
- Sands CJ, McInnes SJ, Marley NJ et al. Phylum Tardigarda: an 'individual' approach. *Cladistics* 2008;24:1–18.
- Som A. Causes, consequences and solutions of phylogenetic incongruence. *Briefings in Bioinformatics* 2015;16:S36–48.
- Stec D, Smolak R, Kaczmarek Ł et al. An integrative description of *Macrobiotus paulinae* sp nov (Tardigrada: Eutardigrada: Macrobiotidae: hufelandi group) from Kenya. *Zootaxa* 2015;4052:501–26.
- Stec D, Morek W, Gąsiorek P et al. Determinants and taxonomic consequences of extreme egg shell variability in *Ramazzottius subanomalus* (Biserov 1985) (Tardigrada). *Zootaxa* 2016;4208:176–88.
- Stec D, Zawierucha K, Michalczyk Ł. An integrative description of *Ramazzottius subanomalus* (Biserov 1985) (Tardigrada) from Poland. *Zootaxa* 2017;4300:403–20.
- Stec D, Morek W, Gąsiorek P et al. Unmasking hidden species diversity within the *Ramazzottius oberhaeuseri* complex with an integrative redescription of the nominal species for the family Ramazzottidae (Tardigrada: Eutardigrada: Parachela). *Systematics and Biodiversity* 2018;16:357–76.
- Stec D, Kristensen RM, Michalczyk Ł. An integrative description of *Minibiotus ioculator* sp. nov. from the Republic of South Africa with notes on *Minibiotus pentannulatus* Londoño et al., 2017 (Tardigrada: Macrobiotidae). *Zoologischer Anzeiger* 2020;286:117–34.
- Streicher JW, Schulte JA, Wiens JJ. How should genes and taxa be sampled for phylogenomic analyses with missing data? An empirical study in iguanian lizards. *Systematic Biology* 2016;65:128–45.
- Surmacz B, Morek W, Michalczyk Ł. What if multiple claw configurations are present in a sample? A case study with the description of *Milnesium pseudotardigradum* sp nov (Tardigrada) with unique developmental variability. *Zoological Studies* 2019;58:32.
- Wiens JJ. Missing data, incomplete taxa, and phylogenetic accuracy. *Systematic Biology* 2003;52:528–38.
- Wiens JJ. Missing data and the design of phylogenetic analyses. *Journal of Biomedical Informatics* 2006;39:34–42.
- Zawierucha K, Stec D, Lachowska-Cierlik D et al. High mitochondrial diversity in a new water bear species (Tardigrada: Eutardigrada) from mountain glaciers in central Asia, with the erection of a new genus *Cryoconicus*. *Annales Zoologici* 2018;68:179–201.
- Zeller C. Untersuchung der phylogenie von Tardigraden anhand der genabschnitte 18S rDNA und cytochrom c oxidase untereinheit I (COXI). M.Sc. Thesis, Wildau (Germany): Technische Hochschule Wildau, 2010.